MAGNETIC MEASUREMENTS OF SESAME STORAGE RING DIPOLES AT ALBA

J. Marcos, V. Massana, J. Campmany,* ALBA-CELLS Synchrotron, Barcelona, Catalonia, Spain,
A. Milanese, C. Petrone, L. Walckiers, CERN, Genève, Switzerland.

Abstract

In this work we present the results of the measurement campaign of the main bending magnets of the SESAME storage ring, which were fully characterized at ALBA-CELLS magnetic measurements facility. A total of 17 combined function dipoles – 16 series magnets plus a pre-series one – has been tested and magnetically measured. This campaign has been performed using a dedicated Hall probe bench. The main measurements included the transfer function at the center of the magnet and field maps of the three components of the field in a plane around the nominal trajectory of the electron beam, at two different operating currents. In this paper we describe the experimental setup and procedures, before reporting the main results, including statistics of magnet-to-magnet reproducibility and integrated field quality. Finally, we show how the measured data can be exploited for an optimal 3D alignment of the dipoles in the machine.

INTRODUCTION

SESAME [1] stands for «Synchro-tron-light for Experimental Science and Applications in the Middle East». It is a cooperative venture by scientists and governments of the region to create a light source in Jordan. SESAME is founded under the auspices of UNESCO and the support of CERN, that took the responsibility of the SESAME storage ring magnets, within the European FP7 project CESSAMag (CERN-EC Support for SESAME Magnets).

The 17 combined function dipoles for SESAME, designed and procured by CERN [2], were manufactured by TESLA Eng. Ltd. (UK). In 2014 ALBA-CELLS signed an agreement with CERN to test and measure all these magnets.

INSTRUMENTS AND METHODOLOGY

ALBA-CELLS task included carrying out the following tests on each magnet:

- resistance and inductance checks
- ground insulation of coils (5 kV) and thermal switches (1 kV) tests
- inter-turn insulation (5 kV) test
- thermal switches performance check
- hydraulic pressure test at 50 bar
- alignment on the bench
- field map and transfer function measurement
- shimming (if required)

For general checks, the instruments used were a Keithley 2010 multimeter, to measure the coil resistance, an Atlas LCR40 from Peak electronic design Ltd., to measure the inductance, a Megger MIT510 to measure the ground insulation, a capacity discharge tester designed and manufactured by Elytt, to measure the inter-turn insulation, and a Rothenberger pressure testing pump.

Alignment has been done using a FARO laser-tracker (Model Xi V2), using the six fiducials on the top, as shown in Figure 1, whose position with respect to the geometrical center of the magnet is known. The position of the sensitive area of the Hall probe is referred to it using a magnet-cone system.

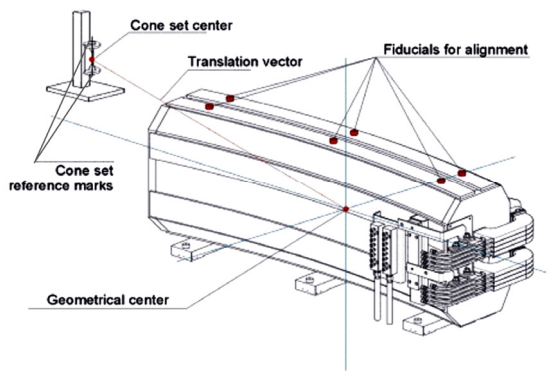

Figure 1: Alignment scheme used to determine the geometrical center of the magnet.

Magnetic measurements have been carried out using the Hall probe bench existing at ALBA along with ancillary reference magnets, described in [3], to achieve a good fiducialization of the physical device with respect to the position and orientation of the Hall probe sensitive areas. The current delivered by the power supply has been also monitored using a DCCT, to correct any drift.

Magnetic measurements for each magnet included the transfer function at its center and field maps at two operating currents, corresponding to injection (0.8 GeV) and nominal (2.5 GeV) electron beam energy.

The transfer function has been determined from transversal scans in the range -40 mm $\leq x \leq$ +40 mm at the center of the dipole, in order to obtain both the magnetic field and the field gradient. Measurements have been carried out for excitation currents spanning from injection energy (154.0 A) up to nominal energy (498.8 A). Hysteresis after decreasing the current down to injection has also been checked.

Field maps have been measured using Hall probe on-the-fly mode along a set of longitudinal lines covering a

ISBN 978-3-95450-147-2

region ±40 mm around the nominal trajectory, as shown in Figure 2. Within the measured region the grid was rectangular with dimensions 2 mm × 4 mm (longitudinal × horizontal).

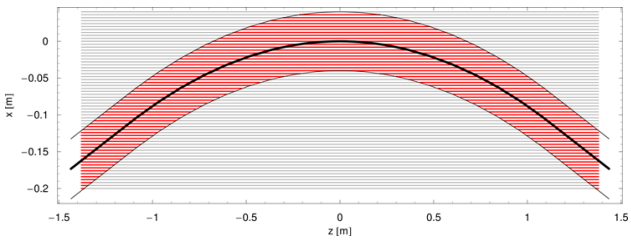

Figure 2: Grid used to measure field maps. It contains circa 18.000 points, and the measurement time is about 3.5 hours. The black line indicates the integration path, and red lines correspond to the scans covering the region ±40 mm at both sides of it.

From field map measurements data has been interpolated along 7 parallel paths at each side of the nominal one, radially separated by 4 mm, and normal and skew components of the magnetic field have been evaluated at each point. Multipoles along a curvilinear coordinate have been extracted from a polynomial fit to the normal / skew field values over adjacent paths. Figure 3 and Figure 4 show as an example the field map and the associated multipoles measured on magnet #17 at nominal energy current.

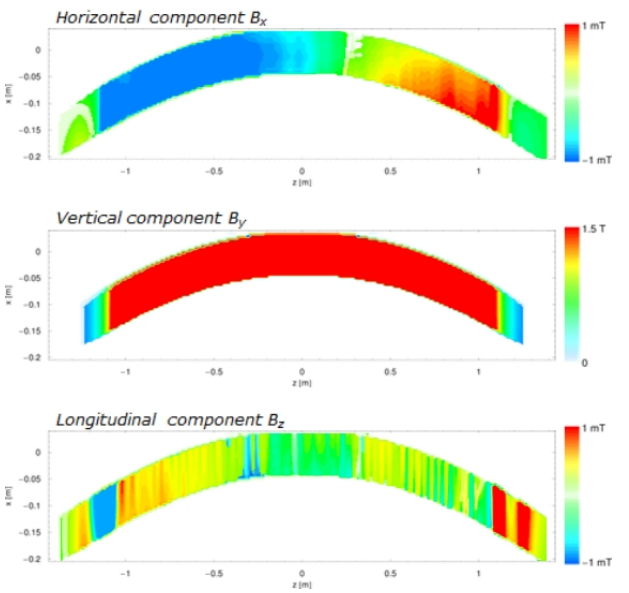

Figure 3: Cartesian components of the magnetic field for SESAME dipole #17 at nominal energy current. Note that color scales are different for B_y (T) than B_x and B_z (mT).

From the obtained multipoles profiles the integrated values have been computed. We have determined that the overall reproducibility of the integrals (taking into account alignment errors, cycling effects, Hall probe noise, etc.) is within $\pm 3 \cdot 10^{-4}$.

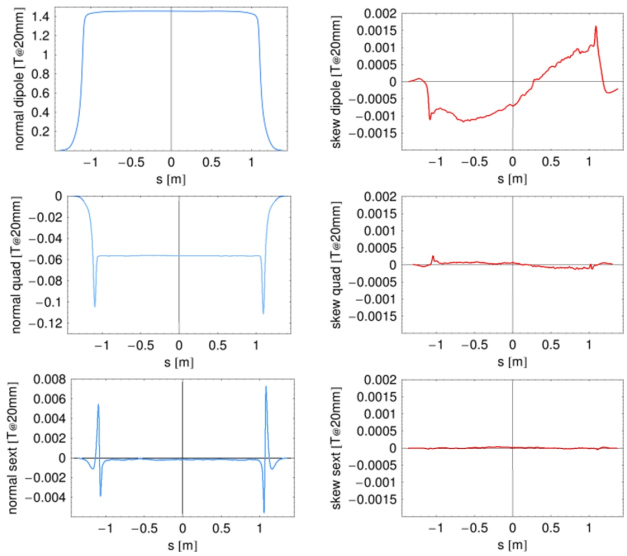

Figure 4: Multipoles along nominal trajectory determined from field map in Figure 3.

The SESAME dipoles are equipped with configurable end shims in order to allow adjusting integrated multipoles magnet-to-magnet. There are three stacks of 1 mm-thick shims which are accommodated in a cut-out of the end plate [2], allowing the integrated field, gradient and sextupole to be adjusted. However, it has been decided not to trim the integrated field deviations, given that they can be easily corrected with a radial displacement. In the case of the integrated gradient, we have adjusted the shim configuration of those magnets displaying deviations larger than $20 \cdot 10^{-4}$: such an adjustment has been required in 9 out of 17 magnets. No deviations of the integrated sextupole requiring correction have been observed.

RESULTS

Figure 5 shows the integrated field homogeneity determined for the dipoles at both injection and nominal energy, compared to the results from Opera-3D simulations. The ΔB/B confirms the choice of the pole width, considering also the sign change –from injection to top energy– due to iron saturation.

Regarding the dispersion of integrated field and gradient values from magnet to magnet, results are shown in Figure 6. The corresponding *rms* values are $\sigma_{\int B}$=1.4‰ and $\sigma_{\int G}$=0.7‰ at nominal energy and $\sigma_{\int B}$=0.7‰ and $\sigma_{\int G}$=1.5‰ at injection, which are within specifications. In the case of the integrated dipole, the dispersion can be set to zero with adequate radial displacements of the magnets.

Figure 7 displays the results for the integrated skew dipole ($\int A_1$) and quadrupole ($\int A_2$): both components have a systematic non-zero value comparable to the maximum strength of the corresponding correctors: 5.3 mT·m for the vertical correctors and 0.9 mT·m for the skew quadrupoles. Therefore these residual skew errors can compromise the flexibility of the accelerator.

ISBN 978-3-95450-147-2

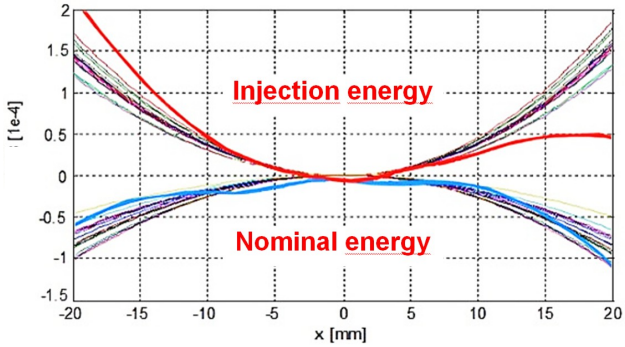

Figure 5: Integrated field homogeneity according to simulations and measurements on 17 dipoles at injection and nominal energy. Red and blue thick lines are the simulations at 2.5 (nominal) and 0.8 GeV (injection).

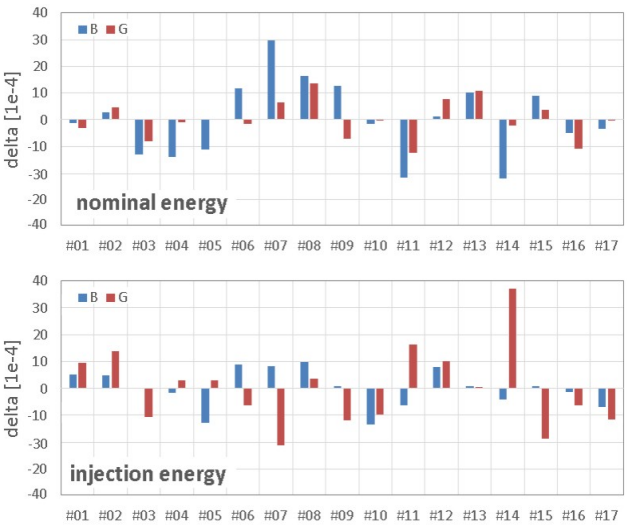

Figure 6: Deviation of integrated field and gradient at nominal and injection energy for all 17 dipoles without optimal alignment.

In order to reduce these components we propose an optimal alignment. For a combined function dipole, $\int A_1$ and $\int A_2$ are sensitive to vertical displacements and roll rotations of the magnet. In fact, given the magnetic field measured in the midplane and making use of Maxwell equations, it is possible to foresee how those components will change when applying a given displacement. By inverting the problem, the displacement (combination of a roll and a vertical shift) required to suppress a given combination of $\int A_1$ and $\int A_2$ values can be deduced.

This correction scheme was successfully tested for one of the dipoles (#11). According to the data obtained at its nominal position, we determined that a roll rotation of 1.72 mrad combined with a vertical displacement of 0.34 mm were required in order to compensate its skew components. The dipole was realigned accordingly and measured again, with a reduction of $\int A_1$ from 8.38 down to 0.13 mT·m and of $\int A_2$ from 0.46 down to 0.03 mT·m (at 20 mm).

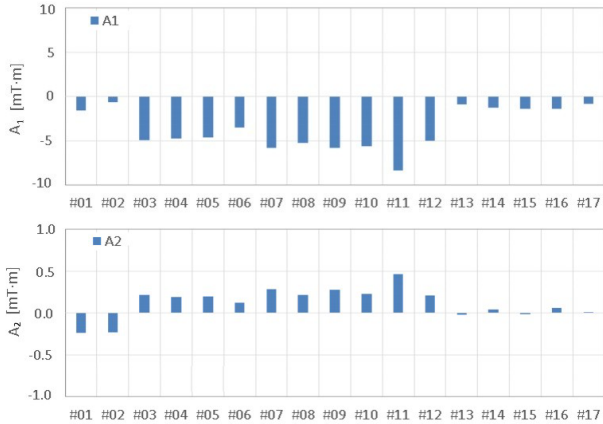

Figure 7: Skew integrated dipole and quadrupole terms at 20 mm of reference radius at nominal energy for all 17 dipoles, without optimal alignment.

CONCLUSION

Data measured during this campaign indicates how the SESAME dipoles shall be positioned and aligned on the girders in order to fit their integrated field and gradient, both normal and skew components. The adjustment of $\int G$ has already been done through the end pole shims; $\int B$ can be fit with a proper radial displacement Δx; finally, $\int A_1$ and $\int A_2$ contributions can be minimized combining a roll rotation with a vertical displacement Δy. This adjustment strategy is illustrated in Figure 8.

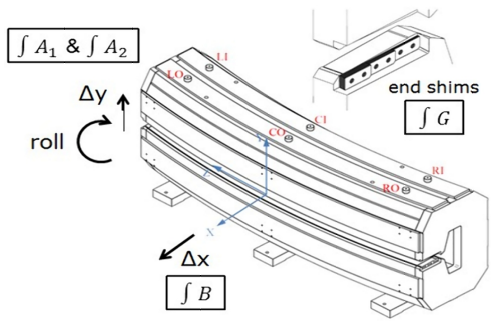

Figure 8: Degrees of freedom to adjust normal / skew integrated field and quadrupole.

ACKNOWLEGDEMENT

This work is supported by the European Commission and CERN under the CESSAMag project, FP7 contract. No. 338602.

REFERENCES

[1] www.sesame.org.jo
[2] A. Milanese, E. Huttel, M. Shehab, "Design of the main magnets of the SESAME Storage Ring," TUPRO105, *Proc. IPAC'15*, Dresden, Germany (2015).
[3] Josep Campmany, Jordi Marcos, Valentí Massana, "New improvements in magnetic measurements laboratory of the ALBA synchrotron facility", *Physics Procedia,* Volume 75, 2015, 1214–1221.